Chapter 6

Effect of Hydroxylation of BT on Dielectric and Mechanical Properties of BMI-Epoxy-BT Nanocomposites

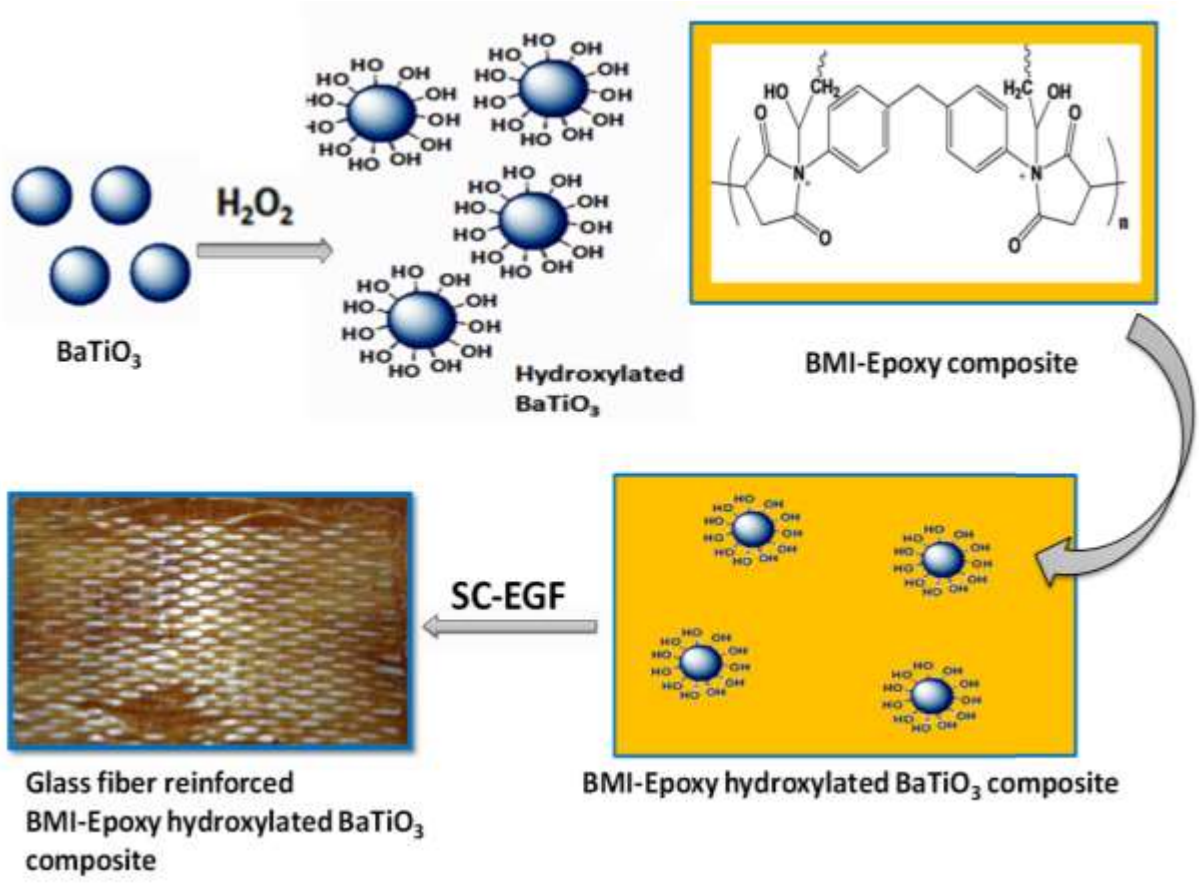

Chapter 6

Effect of Hydroxylation of BT on the Dielectric and Mechanical Properties of BMI-Epoxy-BT Nanocomposites

Abstract

SC-EGF and EGF reinforced BMI-epoxy-hydroxylated $BaTiO_3$ (BTOH) nanocomposites with 1 to 5 weight % of BTOH nanofiller were fabricated by hand layup method and compression moulded. Surface hydroxylation of synthesized $BaTiO_3$ nanoparticles was carried out using H_2O_2. Both BT and BTOH nanoparticles were characterized by SEM, XRD and FTIR studies. SC-EGF reinforced showed a remarkable increase in mechanical and dielectric properties among the reinforced nanocomposites. BMI-epoxy-BTOH nanocomposites with 3 weight % showed highest dielectric strength indicating better insulating properties and composites with 2 weight % of BTOH showed high tensile strength and flexural strength, high dielectric constant and low dielectric loss so that this composition could be explored for high dielectric applications.

6.1 Introduction

Due to the significant improvements in electrical and mechanical properties, polymer nanocomposites have widespread applications in energy storage and microelectronic devices, sensors etc. BMI resin is a novel and promising thermosetting polyimide and this high performance resin finds applications in space ware composites, radar, capacitors, stealth technologies, PCB etc.[1]. They possess excellent oxidative stability, rigidity, thermo-mechanical properties, low moisture absorption, high glass transition temperature, high service temperature stability, retention of physical properties at elevated temperatures as well as in wet conditions. To overcome the brittleness and to improve the processability, BMI resin is blended with epoxy resin. Epoxy resins are used as matrix resins in aerospace composites because of their easy processing, handling convenience, excellent mechanical properties and adhesive nature. Epoxy resins can only be used safely at around 140°C because of their low glass transition temperature[2]. Due to poor hot/wet performance and high moisture sensitivity, they are not used for applications under high temperature conditions. So, blending BMI with

epoxy will be attractive if it results in a matrix with beneficial characteristics of the two constituents.

High dielectric permittivity (k) materials have a wide range of applications in various fields like energy storage capacitors, micro capacitors, sensors, printed circuit boards etc. The incorporation of high k nanofillers into the polymer matrix leads to an increase in the dielectric constant of the polymer nanocomposites. Among the dielectric ceramic particles like Barium titanate (BT), Barium strontium titanate, Boron nitride, Lead zirconate titanate, BT exhibits high dielectric constant and superior properties leading to its widespread usage for matrix reinforcement.

Usually, ferroelectric nanoceramics like BT have poor compatibility with the polymer matrix because of their small size and high surface energy, they are more susceptible to aggregation. This leads to low values of dielectric breakdown owing to an increase in leakage current. Surface functionalization of the filler was the currently employed technique to overcome this problem. Many kinds of research based on the surface modification of the nanofiller were carried out not only to enhance the dielectric properties of the polymer nanocomposites but also to improve the compatibility with the polymer matrix.

There are so many ways to modify the surface of BT nanoparticles such as hydroxylation by H_2O_2[3-8], silanization using different silane coupling agents[3–5], dopamine modification[6], 2,3,4,5-tetrafluorobenzoic acid[7], fluorinated phosphonic acid modification[8], modification with non-ionic and hydrophilic surface agents like polyethylene glycol[9], surface aminated BT nanoparticles[10], chemical modification of the hydroxylated BT nanoparticles using titanate coupling agents[11], modification by ligand exchange reactions[12], by palmitic acid[13], by sodium oleate[14,15]etc. The nanocomposites embedded with these surface hydroxylated and chemically modified nanofillers and nanofibers exhibited remarkable improvement in the dielectric properties which may be ascribed to the enhanced interfacial interaction between the nanoparticles and the polymer matrix thereby increasing the uniform dispersion of nanoparticles with reduced agglomeration. These nanocomposites also exhibit high dielectric permittivity, breakdown strength, low dielectric loss and good compatibility. Among the various chemical modification processes, silanization using silane coupling agents is the most accepted method because further activation of the particle surface can be done by introducing different functional groups into it. The silane coupling

agents are usually added to surface hydroxylated BT nanoparticles (BTOH) because they are more prone to silanization than BT because of the polarity of the former. Current researches reveal that silanization of nanoparticles strongly depends on the reaction kinetics such as reaction time, temperature, different silane coupling agents and solvent effects.

In the present work, surface modification of hydrothermally synthesized BT nanoparticles was carried out by hydroxylation using H_2O_2 treatment. It is the simplest and easiest method for surface modification compared to silanization. The interfacial dipole layer that emerged from the surface hydroxylated BT particles portrays a significant role in the dielectric properties of the fabricated BMI-epoxy composites. As BT lacks reactive functional groups, modification using organic reagents only leads to physisorption on the nanoparticles either by the electrostatic force of attraction or by van der Waal's forces. The synthesized BT nanoparticles contain a low concentration of surface hydroxyl groups and this will not significantly improve the surface activity. For effective modification of BT, more hydroxyl groups are to be produced on the surface of BT nanoparticles that can be attained by treating BT with H_2O_2. Glass fibers were introduced to the bismaleimide-epoxy resin matrix via hand layup method to improve the mechanical properties of the polymer nanocomposites.

6.2 Experimental

6.2.1 Synthesis of hydroxylated barium titanate nanoparticles

Modification of the surface of the synthesized BT nanoparticles was done by treating it with H_2O_2. Firstly, BT nanoparticles and H_2O_2 mixture were ultrasonicated for half an hour. After sonication, the mixture was heated to 106^0C for 5 hours and finally, the obtained hydroxylated BT nanoparticles (BTOH) were filtered and dried at 60^0C for 19 hours[6]. A schematic representation of the synthesis route is given in figure 6.1.

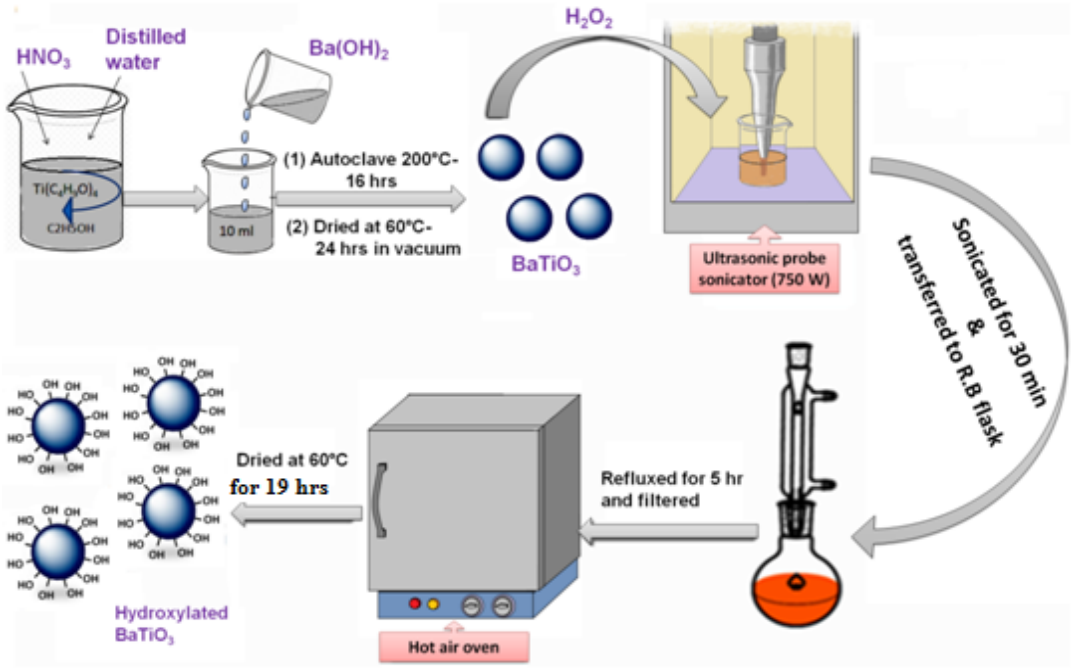

Figure 6.1 Preparation of $BaTiO_3$ (BT) and surface hydroxylated $BaTiO_3$ (BTOH) nanoparticles.

6.3 Results and discussion

6.3.1 Thermogravimetric analysis

From the figure 6.2, it is clear that BMI-epoxy composite with 2 weight % of BTOH nanofiller exhibits better thermal stability compared to cured BMI resin and BMI-epoxy composite. Vapourization of hydroxyl groups grafted onto the surface of BTOH nanoparticles, ie, dehydroxylation that usually occurs in the temperature range 200^{o}C -1000^{o}C[16].

Table 6.1 Tentative assignments from TGA curves of cured BMI resin, BMI-epoxy composite and BMI-epoxy composites with BTOH filler.

Sample	Total weight % at 661°C	T 5% (Initial thermal decomposition temperature)
BMI resin	39	362°C
BMI-epoxy composite without filler	45	368°C
BMI-epoxy composite with 2 weight % of BTOH nanofiller	62.64	392°C

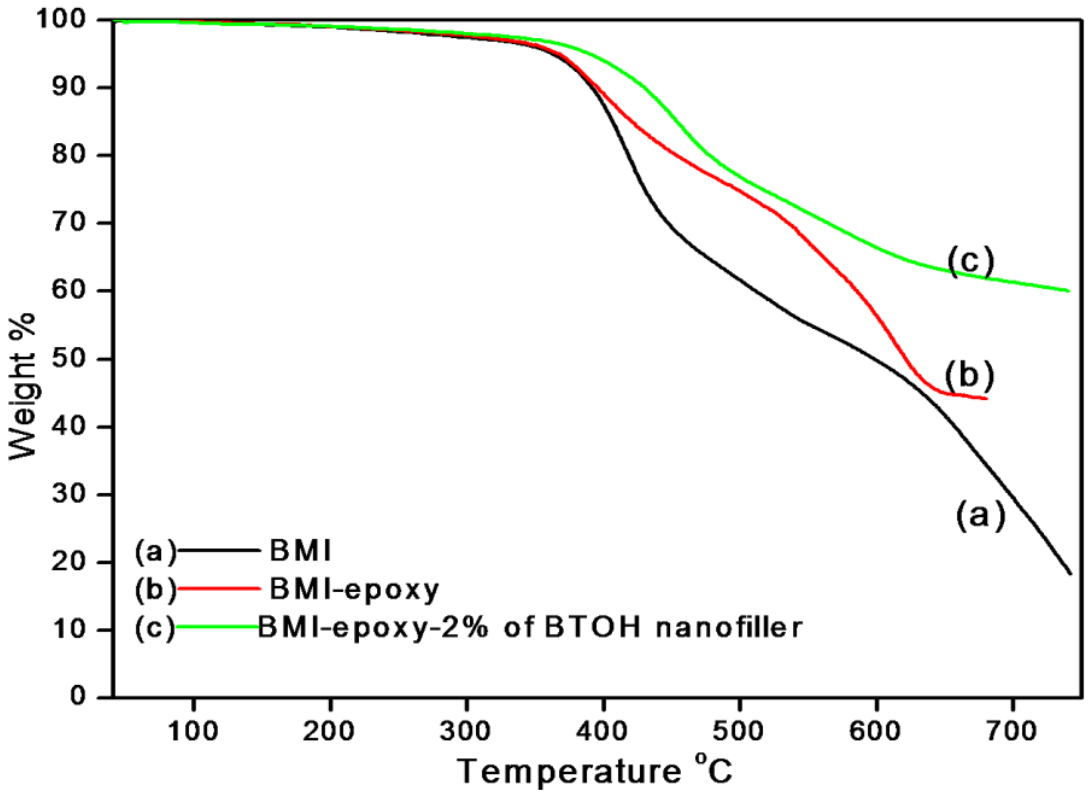

Figure 6.2 TGA curves of (a) BMI resin (b) BMI-epoxy composite without filler and (c) BMI-epoxy composite with 2 weight *% BTOH nanoparticles.*

6.3.2 FTIR analysis

Fourier Transform Infrared spectra of the synthesized BT and BTOH nanoparticles are illustrated in figure 6.3. The absorptions at 637 cm^{-1} in BT and 645 cm^{-1} in BTOH correspond to metal-oxygen (Ti-O) stretching vibrations. Absorptions at 1641 cm^{-1} and 3411 cm^{-1} correspond to the –OH deformations and stretching vibrations respectively, establishing the presence of adsorbed –OH group. A strong peak around 1436 cm^{-1} in both spectra corresponds to C-O stretching vibrations that arose from the carbonate impurity present in BT as $BaCO_3$ in trace quantities during the hydrothermal synthesis[17]. Broadband in the range 3000-3700 cm-1 corresponds to –OH stretching vibrations, confirming the presence of effectively surface hydroxylated BT nanoparticles. The characteristic absorption at 858 cm^{-1} corresponds to Ba-O bond in BT nanoparticles reduced to 855 cm^{-1} in BTOH nanoparticles[9,18].

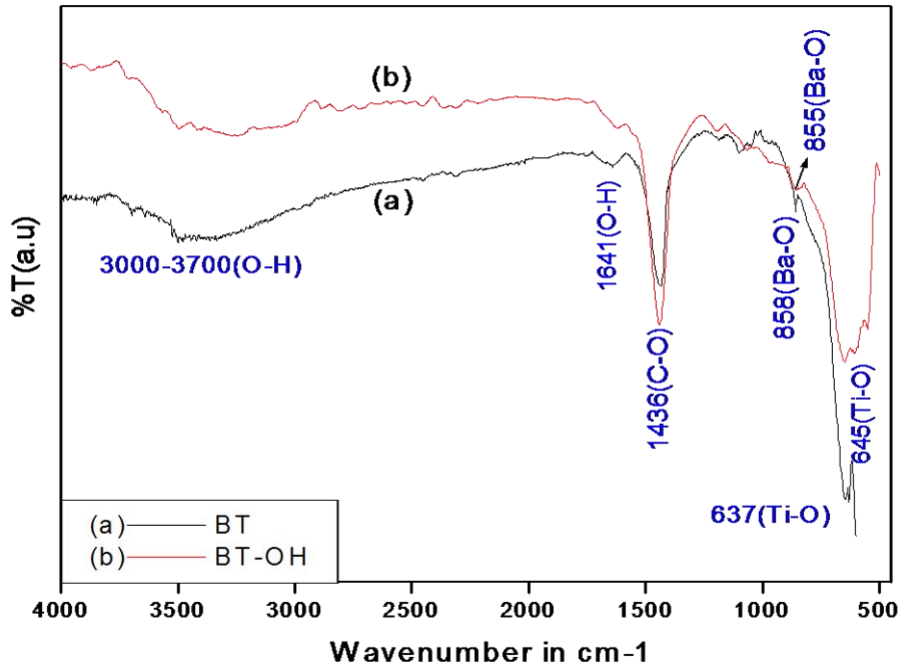

Figure 6.3 FTIR spectra of the synthesized (a) $BaTiO_3$ (b) surface hydroxylated $BaTiO_3$ nanoparticles.

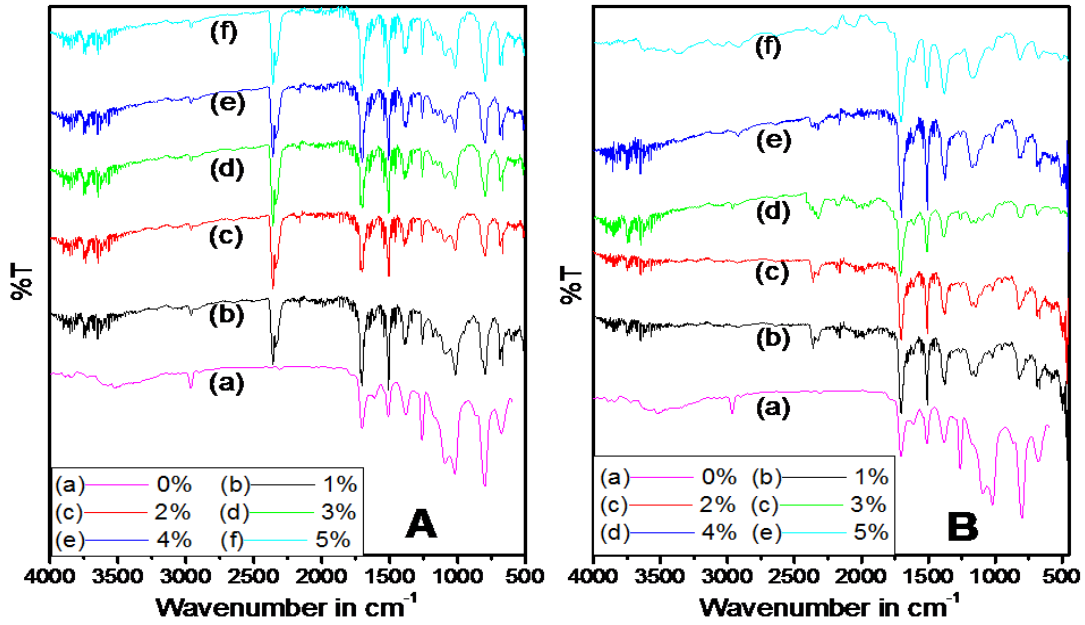

Figure 6.4 FTIR spectra of (A) EGF reinforced and (B) SC–EGF reinforced BMI-epoxy-BTOH nanocomposites.

FTIR spectra of EGF and SC-EGF reinforced BMI-epoxy composites with BTOH loadings in the range from 1 to 5 weight % are illustrated in figure 6.4 A thorough

analysis of the spectra throws light on the fact that the characteristic absorptions are retained in both spectra. Spectral analysis reveals the absorption bands correspond to (i) the maleimide ring and imide group at 686 cm^{-1} and 1382 cm^{-1}, (ii) benzene ring at 820 cm^{-1}, (iii) C-N-C maleimide group around 1094 cm^{-1}, (iv) weak C-N stretch around 1020 $cm^{-1,}$ (v) C=O group at 1710 cm^{-1} and (vi) C=C of benzene ring at 1510 cm^{-1}. The absence of epoxide ring absorption bands at 862, 915, 970 and 1248 cm^{-1} in BMI-epoxy-BTOH nanocomposites is a clear indication of intercrosslinking between bismaleimide and epoxy resin through the opening of the oxirane ring of the epoxy resin (refer figure 4.12, chapter 4). Absorption at 2966 cm^{-1} corresponds to C-H stretching observed in BMI-epoxy composite without nanofiller whereas it is reduced to lower wavenumber in BMI-epoxy-BTOH nanocomposites indicating filler matrix interaction. Absorption at 1386 cm^{-1} corresponds to the imide group, shifted to a lower wavenumber (1382 cm^{-1}) with an increased intensity which may be due to the hydrogen bonding between the hydrogen atoms in BMI-epoxy matrix and oxygen atoms in surface hydroxylated $BaTiO_3$ nanofiller. Each composite also exhibits broadband in the range of 3000-3700 cm^{-1} which indicates the presence of surface hydroxylated BT nanoparticles.

6.3.3 X-ray diffraction Analysis

The perovskite cubic phase of the synthesized BT (figure 6.5 a) was confirmed by XRD analysis. The peaks at 2θ = 22.19º (100), 31.57º (110), 38.92º (111), 45.27º (200), 50.96º (210), 56.18º (211), 65.87º (220), 70.39º (300), 74.82º (310) and 79.17º (311) were consistent with the reported data with JCPDS No#892475.

In X-ray diffractograms of both BT and BTOH nanoparticles, the most intense peak (110) is observed at 2θ values around 31.6°. The peaks at 2θ = 45.15° and 45.3° for BT and BTOH nanoparticles respectively, confirm the presence of the perovskite cubic phase of BT and BTOH[19]. If BT and BTOH nanoparticles were in the tetragonal phase, peaks would split into doublets having 2θ values around 44.8°and 45.4° [20–22].

The similarity in the XRD patterns of BT and BTOH from figure 6.5 reveals that even after refluxing BT nanoparticles with H_2O_2 for 19 hours, crystal structure is not affected and remains intact. Based on the XPS data and zeta potential values, Ohia Chen Li et

al. concluded that during surface hydroxylation of BT nanoparticles, the –OH is attached to barium instead of titanium. This causes the surface of hydroxylated BT to be more Bronsted basic, which may be attributed to the lower ionic potential of barium compared to titanium[6]. H_2O_2 is an reducing agent and it reduces surface oxygen atoms to OH whereas that present in bulk remains as such without undergoing reduction. A comparison of FTIR spectra of BT and BTOH further supports the argument. The bands corresponding to Ba-O vibrations (858 cm^{-1}) were less intense in the spectra of BTOH, whereas more intense O-H stretching vibrations (3700-3000 cm^{-1}) could be observed in BTOH compared to BT.

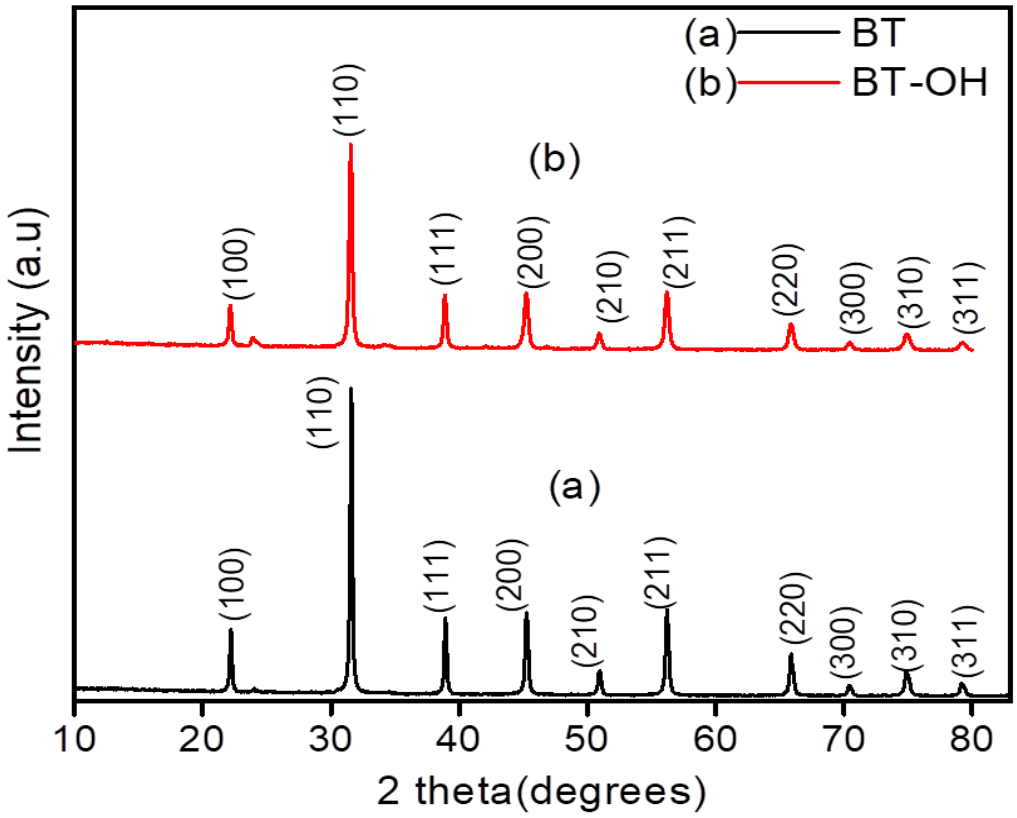

Figure 6.5 Powder XRD patterns of (a) BT nanoparticles (b) BTOH nanoparticles.

The average crystallite size of the BT and BTOH nanoparticles is calculated using Scherrer's formula and is found to be 33 nm and 28 nm respectively.

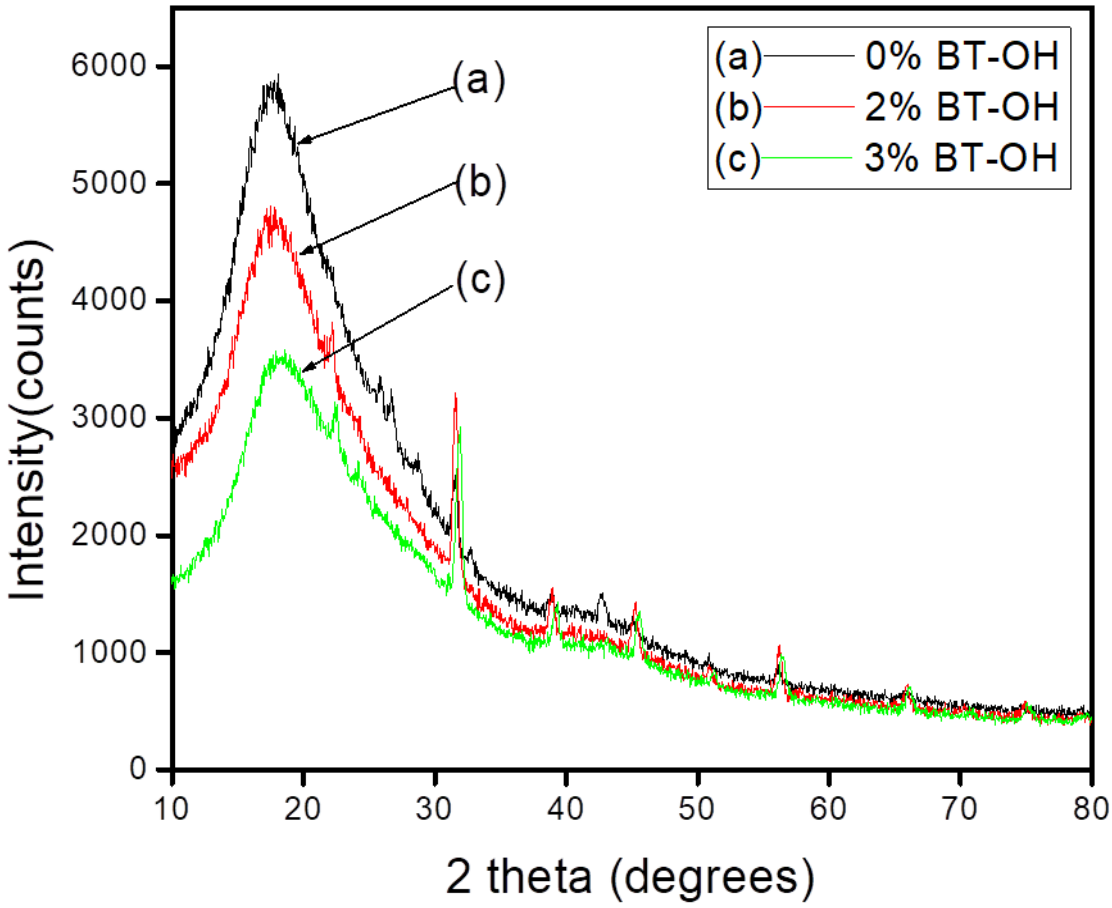

Figure 6.6 Powder XRD patterns of (a) BMI-epoxy composite without BTOH nanofiller and BMI-epoxy composites with (b) 2 weight *% and (c) 3* weight *% BTOH nanofiller.*

No significant shift has happened in the position of the intense peaks at 2θ = 19°-22° corresponding to the incorporation of BTOH nanofiller to BMI-epoxy resin. Sharp crystal peaks corresponding to BTOH nanoparticles were seen in the XRD patterns of the composites. Further analysis of figure 6.6 reveals that the most intense peak of BTOH nanofiller at 2θ value around 32° is retained along with peaks corresponding to the perovskite cubic structure at 2θ value around 45.3°, indicating that the structure of BTOH nanofiller is retained in the BMI-epoxy-BTOH nanocomposite[23].

6.3.4 Morphological studies of BMI-epoxy- BTOH nanocomposites

SEM images reveal the morphology of BTOH (figure 6.7 A), BMI resin (refer chapter 4, section 4.3.2, figure 4.3 B), BMI-epoxy composites with (figure 6.7 B) and without (refer chapter 4, section 4.3.2, figure 4.3 A) BTOH filler. SEM images of BTOH (figure

6.7 A) indicated the existence of BTOH as spherically shaped nanoparticles. Figure 6.7 B represents the SEM image of BMI-epoxy nanocomposite loaded with 2 weight % of BTOH nanoparticles revealing a uniform smooth surface. The phase of embedded BTOH nanoparticles is not much visible in the polymer matrix which supports the uniform dispersion of the former within the matrix.

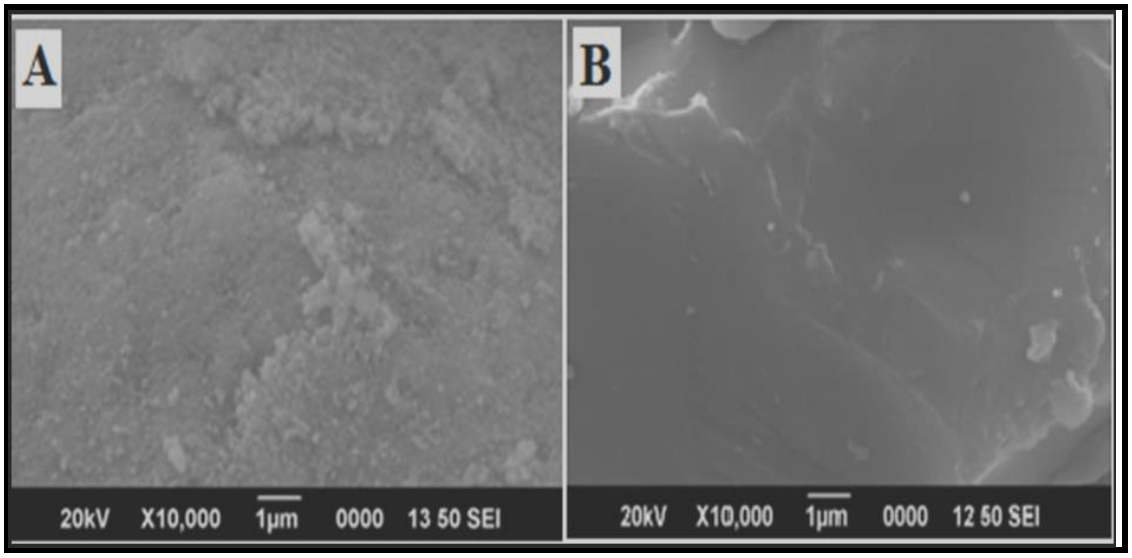

Figure 6.7 SEM images of A) BTOH nanoparticle B) BMI-epoxy composite with 2 weight *% BTOH nanofiller.*

EDAX spectra and mapping images of the synthesized BMI-epoxy composite with 3 weight % of BTOH nanoparticles showed the presence of elements; carbon, oxygen, barium and titanium along with their dispersion in the composite matrix (figure 6.8). The presence of chlorine atoms in traces, as an impurity, observed in the EDAX spectra of BMI-epoxy-BTOH nanocomposite might have originated from the BMI since the EDAX of BTOH is free of chlorine (figure 6.9). The EDAX pattern hence shows the presence of all the elements as expected for bismaleimide-epoxy-BTOH nanocomposites.

EDAX analysis of the synthesized BTOH nanoparticles (figure 6.9) confirmed that there were no impurities in the sample and has a composition of barium ≈65%, titanium ≈17% and oxygen ≈18%.

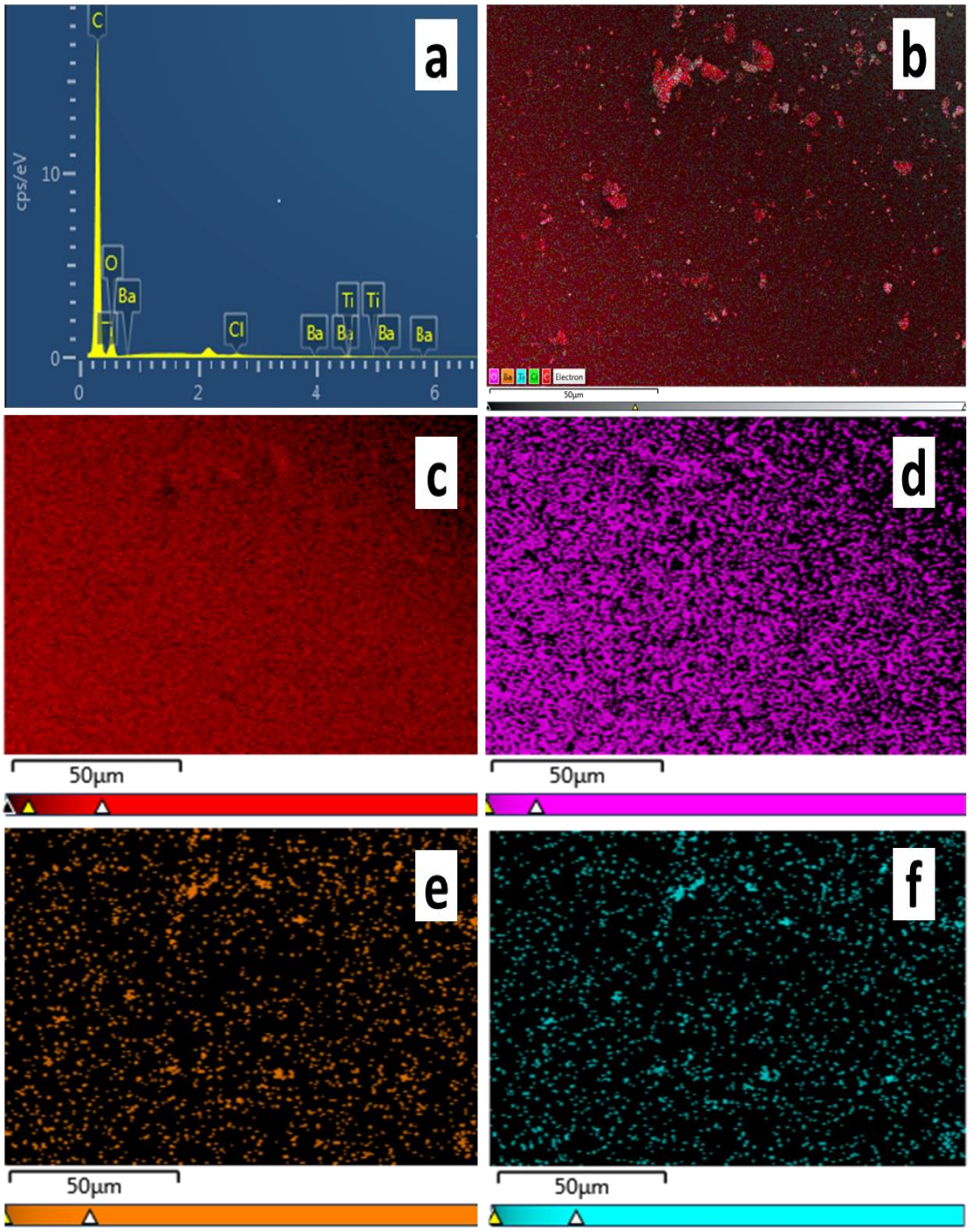

Figure 6.8 EDAX spectra (a) and EDAX mapping (b) of BMI-epoxy composite with 3 weight % BTOH. EDAX mapping of carbon (c), oxygen (d), barium (e) and titanium (f).

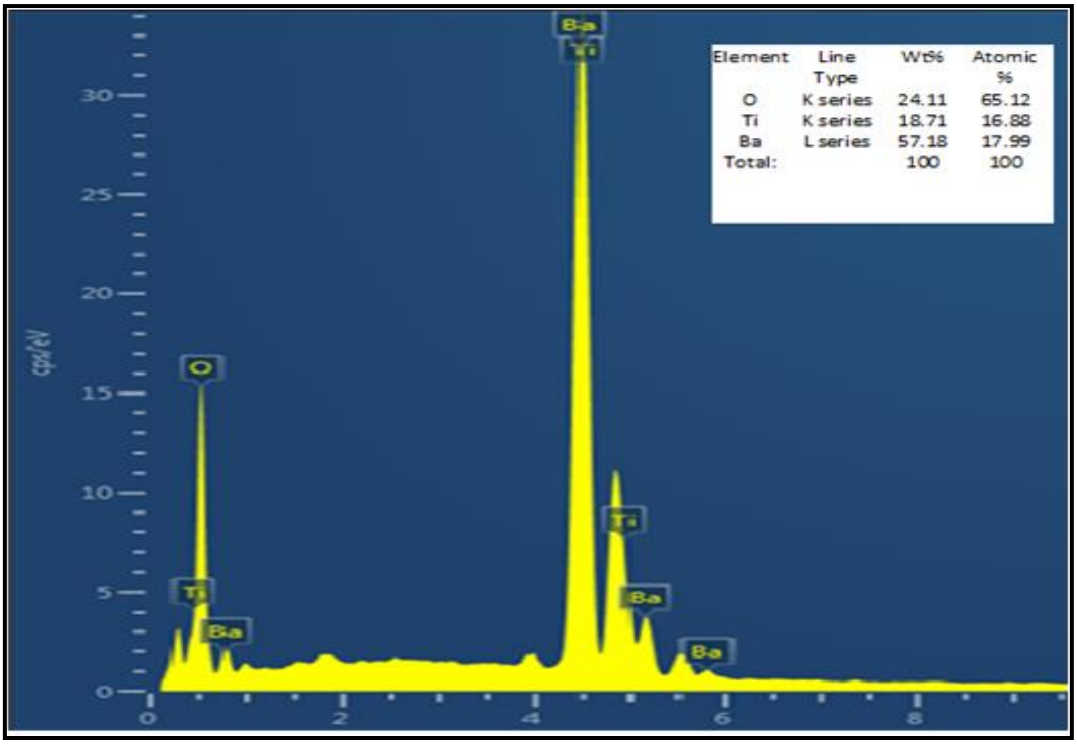

Figure 6.9 *EDAX of BTOH nanoparticles.*

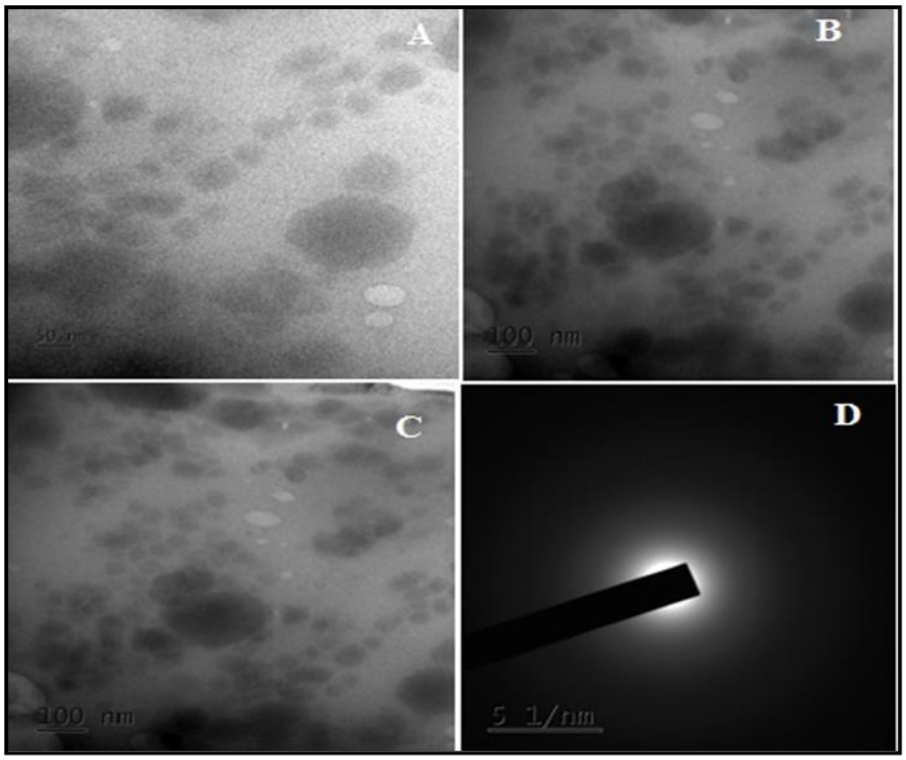

Figure 6.10 TEM (figure A, B and C) and SAED (figure D) images of BMI-epoxy nanocomposites with 3 weight % of BTOH nanofiller without EGF or SC-EGF reinforcement.

In order to study the dispersion of BTOH, TEM and SAED images of BMI-epoxy composites with 3 weight % of BTOH nanofiller were also taken. From figure 6.10 (A, B and C), it is evident that BTOH nanofiller was homogeneously distributed without any agglomeration. The brighter spherical parts may indicate glass fibers that were unknowingly present during the powdering of the sample. SAED pattern of the composite showed no clear spots or distinct ring patterns. The foggy type SAED pattern reveals the amorphous nature of BMI-epoxy-BTOH nanocomposite (figure 6.10 D).

6.3.5. Mechanical properties of BMI-epoxy-BTOH nanocomposites

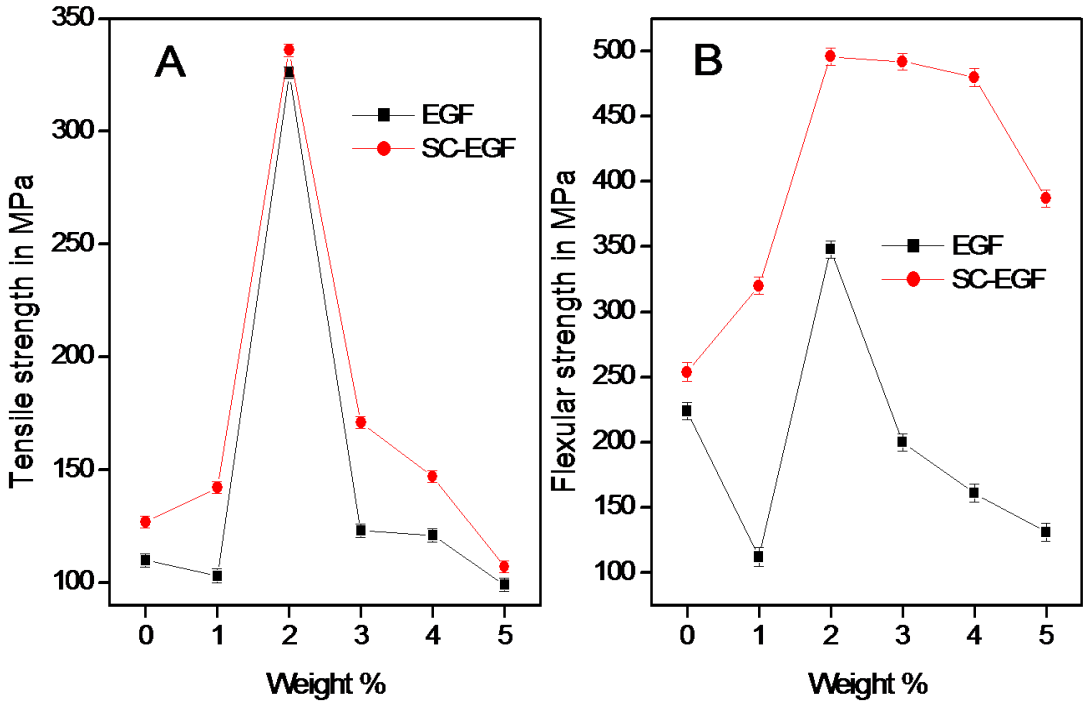

Figure 6.11 Influence of weight % of BTOH nanoparticles on (A) tensile strength and (B) flexural strength of BMI-epoxy-BTOH nanocomposites with EGF and SC-EGF as reinforcement.

Figure 6.11 represents the result of flexural and tensile measurements of the BMI-epoxy-BTOH nanocomposites done as per ASTM standards. It is evident from the figure that for the BMI-epoxy-BTOH nanocomposites, the mechanical properties such as flexural strength and tensile strength increase with BTOH percentage, reaching a maximum value at 2 weight % and thereafter decreases. 2 weight % BTOH loading could therefore be considered optimum in order to achieve maximum

mechanical strength for BMI-epoxy-BTOH nanocomposite. Above 2 weight % loading, BTOH nanoparticles agglomerate within the matrix leading to a drop in its mechanical strength. The enhancement in the mechanical properties when compared with barium titanate incorporated BMI-epoxy matrix may be due to the surface hydroxylation of BT nanoparticles which results in a high degree of matrix interaction and uniform dispersion of nanoparticles in the polymer matrix[29-32]. It is established from the test results that due to greater interaction between SC-EGF and BMI-epoxy matrix there is a significant enhancement in both tensile and flexural strength of BMI-epoxy-BTOH nanocomposites reinforced with SC-EGF compared to composites with EGF reinforcement[33].

6.3.6. Dielectric properties of BMI-epoxy-BTOH nanocomposites

6.3.6.1 Dielectric permittivity

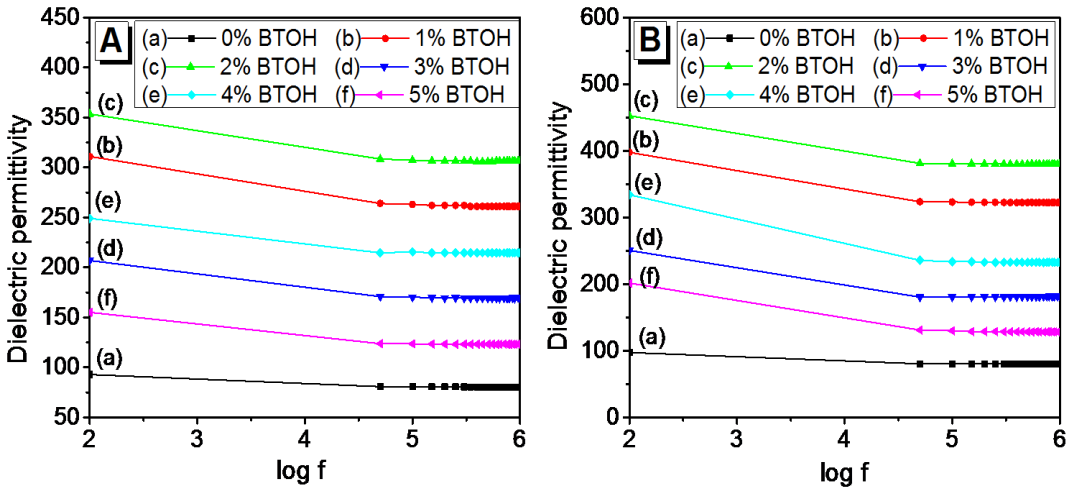

Figure 6.12 Plots of frequency versus dielectric permittivity of BMI-epoxy-BTOH nanocomposites with (A) EGF (B) SC-EGF as reinforcement.

Figure 6.12 represents the dielectric constant versus frequency plots of BMI-epoxy-BTOH nanocomposites with 1-5 weight % loadings of BTOH nanofiller. The maximum value of dielectric permittivity was obtained at 2 weight % BTOH loading in BMI-epoxy nanocomposites reinforced with SC-EGF and EGF. The functionalization of BT by surface hydroxylation improves the interfacial interaction between the BTOH nanoparticle and BMI-epoxy resin matrix thereby increasing the dispersion of BTOH

nanofiller in the BMI-epoxy resin matrix resulting in higher dielectric constant values for the composites[8,37,34].

6.3.6.2 Dielectric loss (tan delta)

Figure 6.13 shows the variation of dielectric loss **(**tan delta) with the applied frequency of BMI-epoxy composites for differently loaded BTOH nanoparticles. Upto 2 weight % of BTOH nanoparticles, tan δ of composites remained very low.

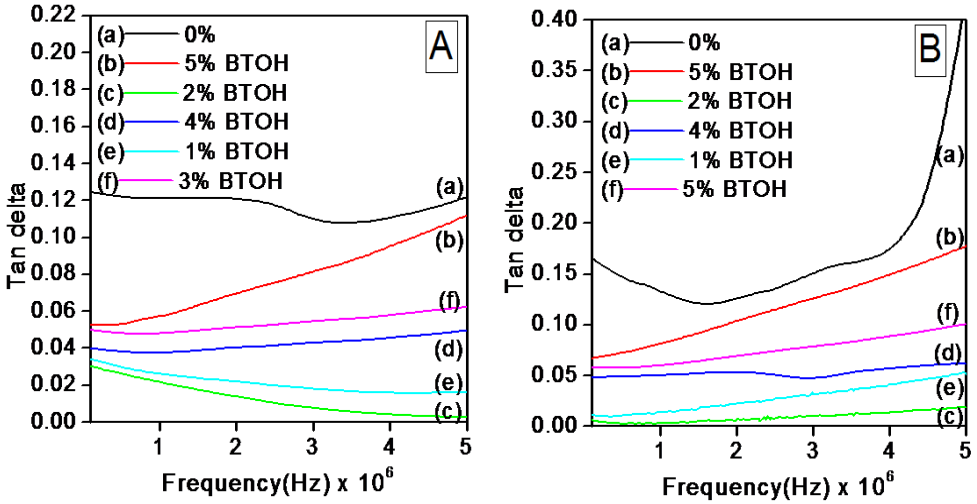

Figure 6.13 Plots of frequency-tan delta of BMI-epoxy-BTOH nanocomposites with (A) EGF (B) SC-EGF as reinforcement.

6.3.6.3 Dielectric Strength

The characteristic dielectric strength of BMI-epoxy-BTOH nanocomposites is illustrated in figure 6.14. The energy storage capacity of polymer nanocomposites depends on the magnitude of dielectric strength. All of the BMI-epoxy-BTOH nanocomposites withstand low AC electric field tests over 2-6 kV/mm, performed as per ASTM standard D149. At first, dielectric strength increases with an increase in weight percentage of BTOH upto 3 weight % for both EGF and SC-EGF BMI-epoxy-BTOH nanocomposite which again may be due to the increased interfacial interaction and uniform distribution of nanoparticles[4,35,36] and then decreases, which may be due to the nonuniform particle dispersion caused by the agglomeration of nanoparticles and voids created inside the polymer matrix.

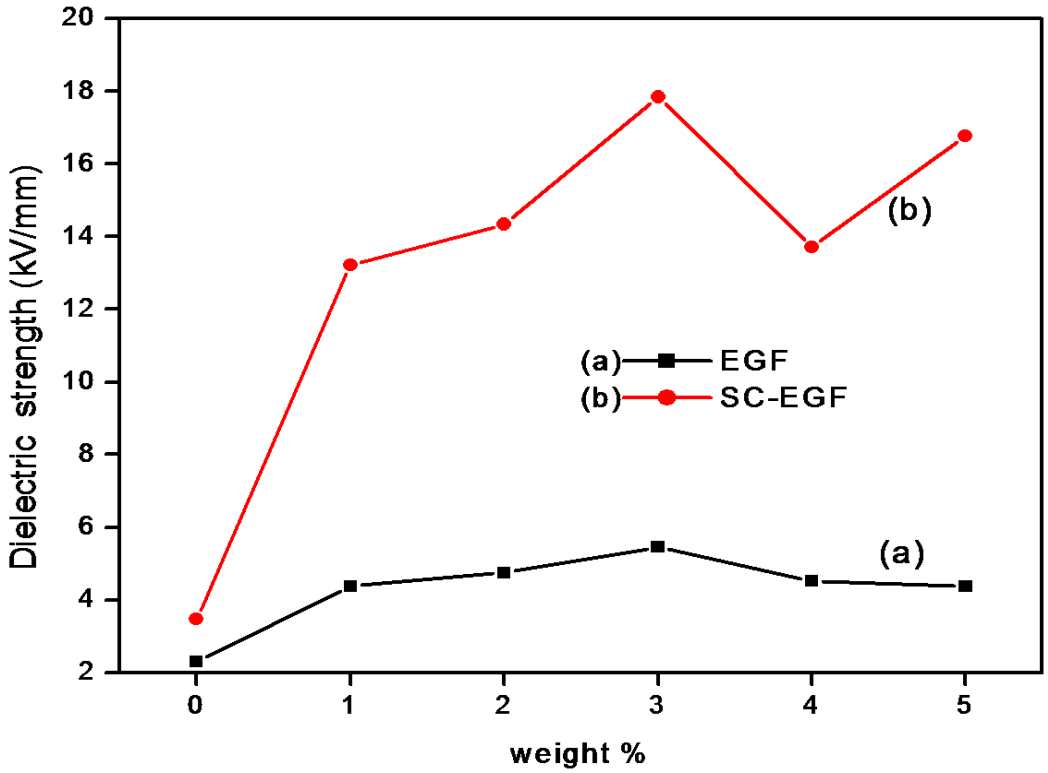

Figure 6.14 Effect of weight % of BTOH nanoparticles on dielectric strength of BMI-epoxy-BTOH nanocomposites.

6.4 Conclusions

Surface modification of barium titanate (BT) nanoparticles was done using H_2O_2. XRD patterns confirm surface hydroxylation of BT nanofillers and FTIR spectra support effective surface hydroxylation. The modified BT nanoparticles (BTOH) were used to prepare glass fiber reinforced BMI-epoxy nanocomposites with 1-5 weight % BTOH loadings. The effect of BTOH nanoparticles on the mechanical and dielectric properties of BMI-epoxy nanocomposites was studied. Tensile strength of BMI-epoxy composite with 2 weight % BTOH nanoparticles was increased 2.97 and 3.34 times both in EGF and SC-EGF reinforced composites whereas the flexural strength of the above composite was increased 1.55 and 1.95 times respectively with EGF and SC-EGF reinforcement as compared to the BMI-epoxy composite without filler. The remarkable enhancement in both mechanical as well as dielectric properties may be attributed to the enhanced interfacial interaction between the polymer matrix and BTOH nanofiller. Above 2 weight % concentration, there is a chance for filler aggregation so that uniform dispersion would not be possible which leads to a

reduction in both mechanical as well as dielectric properties. Both E-glass fiber and silane coated E-glass fiber reinforced BMI-epoxy-BTOH nanocomposite with 3 weight % of BTOH exhibit better insulating properties and composites with 2 weight % exhibited maximum dielectric constant and low dielectric loss values along with enhancement in mechanical properties making this composition more suitable for high dielectric applications.

References

1. Fernandes, E. G., Tramidi, C., Gregorio, G. M. Di & Angeloni, G. Effect of Temperature-Pressure Cycles on Structural Properties of Epoxy-Based Composites for Printed Circuit Boards Applications. Appl. Polym. Sci. 110, 1606–1612 (2008).
2. Landman, D. Advances in the Chemistry and Applications of Bismaleimides BT - Developments in Reinforced Plastics—5: Processing and Fabrication. in (ed. Pritchard, G.) 39–81 (Springer Netherlands, 1986). doi:10.1007/978-94-009-4179-3_2.
3. Fan, Y. et al. Applied Surface Science Molecular structures of (3-aminopropyl) trialkoxysilane on hydroxylated barium titanate nanoparticle surfaces induced by different solvents and their effect on electrical properties of barium titanate based polymer nanocomposites. Appl. Surf. Sci. 364, 798–807 (2016).
4. Kamezawa, N., Nagao, D., Ishii, H. & Konno, M. Transparent, highly dielectric poly (vinylidene fluoride) nanocomposite film homogeneously incorporating $BaTiO_3$ nanoparticles with fluoroalkyl silane surface modifier. Eur. Polym. J. (2015) doi:10.1016/j.eurpolymj.2015.03.021.
5. Zhang, X., Ma, Y., Zhao, C. & Yang, W. Applied Surface Science High dielectric constant and low dielectric loss hybrid nanocomposites fabricated with ferroelectric polymer matrix and $BaTiO_3$ nanofibers modified with perfluoroalkyl silane. Appl. Surf. Sci. 305, 531–538 (2014).
6. Song, Y. et al. Enhanced dielectric and ferroelectric properties induced by dopamine-modified $BaTiO_3$ nanofibers in flexible poly(vinylidene fluoride-trifluoroethylene) nanocomposites. J. Mater. Chem. 22, 8063–8068 (2012).
7. Yujuan Niu, Ke Yu, Yuanyuan Bai, Feng Xiang, H. W. Fluorocarboxylic acid modified Barium Titanate/poly(vinylidene fluoride) composite with significantly enhanced breakdown strength and high energy density. RSC Adv. (2015) doi:10.1039/b000000x.
8. Kim, P. et al. High Energy Density Nanocomposites Based on Surface-Modified $BaTiO_3$ and a Ferroelectric Polymer. ACS Nano 3, 2581–2592 (2009).
9. Moharana, S., Mishra, M. K., Behera, B. & Mahaling, R. N. Enhanced Dielectric Properties of Polyethylene Glycol (PEG) Modified $BaTiO_3$ (BT) -Poly (vinylidene fluoride) (PVDF). Polym. Sci. A 59, 405–415 (2017).
10. Zhao, Y., Seah, L. K. & Chai, G. B. Long-Term Viscoelastic Response of E-glass / Bismaleimide Composite in Seawater Environment Long-Term Viscoelastic Response of E-glass / Bismaleimide Composite in Seawater Environment. Appl. Compos. Mater. 22, 693–709 (2015).
11. Hu, P., Gao, S., Zhang, Y., Zhang, L. & Wang, C. Surface modified $BaTiO_3$ nanoparticles by titanate coupling agent induce significantly enhanced breakdown strength and larger energy density in PVDF nanocomposite. Compos. Sci. Technol. 156, 109–116 (2018).
12. Kim, Y. et al. Highly Fluorinated Polymer-Inorganic Nanoparticle Composites Processable with Fluorous Solvents. J. Nanosci. Nanotechnol. 17, 5510–5514 (2017).
13. Piana, F. One-pot preparation of surface-functionalized barium titanate nanoparticles

for high-K polystyrene composite films prepared via floating method. J. Mater. Sci. 53, 11343–11354 (2018).
14. Chang, S., Liao, W., Ciou, C., Lee, J. & Li, C. An efficient approach to derive hydroxyl groups on the surface of barium titanate nanoparticles to improve its chemical modification ability. J. Colloid Interface Sci. 329, 300–305 (2009).
15. Nikita, E. Structure and dielectric properties of composite material based on surface-modified $BaTiO_3$ nanoparticles in polystyrene. Eur.Phys.J.Appl.Phys 69, (2015).
16. Ahmari, S. & Zhang, L. The properties and durability of mine tailings-based geopolymeric masonry blocks. Eco-efficient Masonry Bricks and Blocks: Design, Properties and Durability (Elsevier Ltd, 2014). doi:10.1016/B978-1-78242-305-8.00013-9.
17. Mai, T. T. et al. Enhancement of polarization property of silane-modified $BaTiO_3$ nanoparticles and its effect in increasing dielectric property of epoxy/$BaTiO_3$ nanocomposites. J. Sci. Adv. Mater. Devices 1, 90–97 (2016).
18. Asimakopoulos, I. A., Psarras, G. C. & Zoumpoulakis, L. Barium titanate/polyester resin nanocomposites : Development, structure-properties relationship and energy storage capability. Express Polym. Lett. 8, 692–707 (2014).
19. Tao, J., Ma, J., Wang, Y. & Zhu, X. Synthesis of barium titanate nanoparticles via a novel electrochemical route. Mater. Res. Bull. 43, 639–644 (2008).
20. Chen, D. & Luo, Y. The influence of anions on the products of $BaTiO_3$ under hydrothermal conditions. J. Mater. Sci. 31, 6201–6205 (1996).
21. Xia, C., Shi, E., Zhong, W. & Guo, J. Preparation of $BaTiO_3$, by the Hydrothermal Method. 2219, 1171–1176 (1995).
22. Dutta, P. K., Asiaie, R., Akbar, S. A. & Zhug, W. Hydrothermal Synthesis and Dielectric Properties of Tetragonal BaTiOs. Chem. Mater. 6, 1542–1548 (1994).
23. Upc, D. & González, N. Improvement of Insulation Effectiveness of Natural Rubber by Adding Hydroxyl-Functionalized Barium Titanate. IEEE Trans. Dielectr. Electr. Insul. 24, 2881–2889 (2017).
24. Choudhury, A. Preparation, characterization and dielectric properties of polyetherimide nanocomposites containing surface-functionalized $BaTiO_3$ nanoparticles. Polymer Int. 61(5), 696–702 (2012).
25. Mei Dub, Wei Wanga, Lei Chena, Zhiwei Xua, Hongjun Fua, and M. M. Enhancing Dielectric Properties of Poly(vinylidene fluoride)-Based Hybrid Nanocomposites by Synergic Employment of Hydroxylated $BaTiO_3$ and Silanized Graphene. Polym. - Plastics Technol. Eng. 55, 1595–1603 (2016).